International Journal of Applied Mechanics
Vol. 8, No. 7 (2016) 1640009 (16 pages)

DOI: 10.1142/S1758825116400093

World Scientific
www.worldscientific.com

Modal Analyses of Deployable Truss Structures Based on Shape Memory Polymer Composites

Fengfeng Li*, Liwu Liu*, Xin Lan†, Tong Wang*,‡, Xiangyu Li*, Fanlong Chen*, Wenfeng Bian‡, Yanju Liu*,§ and Jinsong Leng†

*Department of Astronautical Science and Mechanics
Harbin Institute of Technology, Harbin 150001, P. R. China

†Centre for Composite Materials and Structures
Harbin Institute of Technology, Harbin 150080, P. R. China

‡Department of Civil Engineering
Harbin Institute of Technology (Weihai)
Weihai 264200, P. R. China
§yj_liu@hit.edu.cn

Received 16 August 2016
Revised 10 October 2016
Accepted 11 October 2016
Published 30 December 2016

With large spatial deployable antennas used more widely, the stability of deployable antennas is attracting more attention. The form of the support structure is an important factor of the antenna's natural frequency, which is essential to study to prevent the resonance. The deployable truss structures based on shape memory polymer composites (SMPCs) have made themselves feasible for their unique properties such as highly reliable, low-cost, light weight, and self-deployment without complex mechanical devices compared with conventional deployable masts. This study offers deliverables as follows: an establishment of three-longeron beam and three-longeron truss finite element models by using ABAQUS; calculation of natural frequencies and vibration modes; parameter studies for influence on their dynamic properties; manufacture of a three-longeron truss based on SMPC, and modal test of the three-longeron truss. The results show that modal test and finite element simulation fit well.

Keywords: Shape memory polymer composites; three-longeron beam; three-longeron truss; finite element simulation; modal test.

1. Introduction

Shape memory polymer (SMP) is a kind of macromolecular smart material that can respond to external stimulus (heat, electricity, magnetism, light, moisture, etc.) by changing its macroscopic properties (shape, color, etc.) and then recovering to its original shape from its temporary shape [Behl and Lendlein, 2007; Behl *et al.*, 2010; Hu *et al.*, 2012; Kunzelman *et al.*, 2008; Leng *et al.*, 2009, 2011; Mather *et al.*, 2009; Ratna and Karger-Kocsis, 2008; Xie, 2010]. For a better understanding on the shape memory effect of SMP, here take thermal-responsive SMP as an example.

The shape memory process is divided into four steps: (a) Heat the material to above transition temperature and deform the material with external force; (b) cool the material to below transition temperature under constraint; (c) hold the temperature below transition temperature, then remove the constraint to get the fixed shape; (d) reheat the deformed material to above transition temperature to get the original shape of the material. However, SMPs also have some inherent drawbacks, such as low deformation stiffness and low recovery stress [Lv *et al.*, 2010; Ohki *et al.*, 2004; Wei *et al.*, 1998]. To overcome these deficiencies, shape memory polymer composites (SMPCs) have been developed to satisfy demands in practical applications. SMPCs have higher strength, higher stiffness and certain special characteristics determined by which fillers are added [Basit *et al.*, 2013; Choi *et al.*, 2012; Gunes and Jana, 2008; Leng *et al.*, 2011; Meng and Hu, 2009; Ratna and Karger-Kocsis, 2008; Zhou and Liu, 2009].

When the carrying capability of rockets is considered, deployable structures are a practical way to construct large, lightweight structures for space applications [Gunnar, 2002; Liu *et al.*, 2014; Richard, 1995]. The typical deployable structures are mast, antenna, space telescope, solar array, and solar sail, etc. [Brown, 2011; Ercol *et al.*, 2000; Feng, 2006; Gunnar, 2002; Hanayama *et al.*, 2004; Im *et al.*, 2007; Keller *et al.*, 2004; Lillie, 2005; Luo and Duan, 2005; Mori *et al.*, 2009; Oegerle *et al.*, 2006; Takano *et al.*, 2004; Tsuda *et al.*, 2013; Wie *et al.*, 1986].

Masts are usually used for supporting other structures such as antenna, solar array [Brown, 2011; Feng, 2006]. The conventional deployment approaches for mast are cable-activated and spindle-and-nut techniques, which means electric motor and reel devices are needed. This kind of deployment is reliable but adds complexity to the mast [Gunnar, 2002; Keller *et al.*, 2004]. Nowadays, there exists several deployable masts which have simple structures but still need mechanical devices for storage and release, they can be divided into articulated trusses, coilable trusses, and storable tubular extendible member booms, etc. [Campbell *et al.*, 2005; Keller *et al.*, 2004; Li *et al.*, 2016; Liu *et al.*, 2014; Pollard *et al.*, 2007; Zhang *et al.*, 2014]. The deployable masts based on SMPC have made themselves feasible because of their light weight, simple mechanical design, low-cost, reliable driving components which are made of SMPC [Fetchko *et al.*, 2004; Li *et al.*, 2016; Zhang *et al.*, 2014].

One of the design principles of masts is high stiffness-to-weight ratio. The high stiffness of support structure can ensure the payload has a relatively high first-order natural frequency. The deployable truss structures in this study are mainly designed for supporting antennas whose surface accuracy is extremely sensitive to its flexibility [Brown, 2011; Feng, 2006; Gunnar, 2002; Keller *et al.*, 2004]. Since the support structure is an important factor of the antenna's vibration it is necessary to study the dynamic characteristics of the form of support structure to find out the main factors resulting in its vibration, thus avoiding the resonance which leads to the damage of the antenna.

This paper develops three-longeron beam and three-longeron truss structures by using the arc-shaped deformable shells which are made of carbon fiber reinforced

epoxy-based SMPC. ABAQUS package is adopted to establish the two kinds of models, and the detailed parameter studies of the factors affecting the natural frequency of them are carried out. Moreover, the three-longeron truss structure is manufactured, its modal is conducted. The results show that modal test and finite element simulation results fit well.

2. The Modal Analysis of the Three-Longeron Beam

The three-longeron beam consists of three parts: sleeves group, supporting components group, and arc-shaped deformable shells group. The intermediate shaft of the structure is the extensible sleeves. The arc-shaped deformable shells are all placed around the sleeves, the shells are connected by components. The arc-shaped deformable shells are the main part of the beam and they are fabricated with carbon fiber reinforced epoxy-based SMPC, the material is the same as that in Zhang *et al.* [2014]. A resistor heater is stuck to the surface of every arc-shaped deformable shell, since the SMP used here is thermal-responsive material. The deformable shells are packaged into a 'V-shape' firstly; when the resistor heaters are electrified, the shells deploy gradually with time, providing an increase in driving force to unfold the packaged beam.

According to the actual physical model which we have, the arc-shaped deformable shells are established, whose central angle is 90°, radius is 25 mm, thickness is 2 mm, and length is 300 mm. A local cylinder coordinate is established in the center of the shell. Then material direction of composite layer is arranged by the local cylinder coordinate system (as shown in Fig. 1). The material is simplified as regular symmetric cross-ply laminates. The parameters of the unidirectional carbon fiber reinforced epoxy-based composite are shown in Table 1. The density is $\rho = 1.5E - 9t/\text{mm}^3$. The composite shell is composed of four layers, each layer's thickness is 0.5 mm. The principle directions are defined in cylinder coordinate, and the ply methods of carbon fiber reinforced epoxy-based SMPC are shown in Table 2.

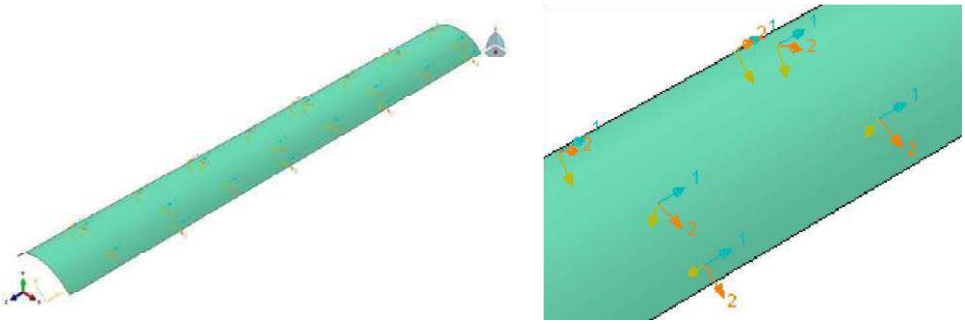

Fig. 1. Material direction of composite material layer.

Table 1. Material parameters of unidirectional carbon fiber reinforced epoxy-based SMPC.

E1 (MPa)	E2 (MPa)	Nu12	G12 (MPa)	G13 (MPa)	G23 (MPa)
30,000	2800	0.4	1500	1000	1000

Table 2. Ply methods of carbon fiber reinforced epoxy-based SMPC.

Material	Thickness (mm)	Orientation angle (°)
Material-SMPC	0.5	0
Material-SMPC	0.5	90
Material-SMPC	0.5	0
Material-SMPC	0.5	90

Table 3. Parameters of sleeves group.

Parameter	The first part	The second part	The third part	The fourth part
The length (mm)	630	570	570	570
Outer diameter (mm)	18	16	14	12
Inner diameter (mm)	16	14	12	10

The sleeves and supporting components of three-longeron beam are all established by solid parts. The sleeves group includes four parts, and the parameters of each part are shown in Table 3. Furthermore, there are seven supporting components to connect the arc-shaped deformable shells. Supporting components are attached to the sleeves, and their locations along the axial direction of the sleeves are 100, 420, 740, 1060, 1380, 1700 and 2020, respectively.

The material parameters of sleeves made by fiber reinforced plastic (FRP) are shown as follows:

$$\text{Elasticity modulus: } E = 21{,}000\,\text{MPa},$$

$$\text{Poisson ratio: } \nu = 0.3, \quad \text{density: } \rho = 1.08E - 9t/\text{mm}^3.$$

The material parameters of supporting components made by aluminum alloy are shown as follows:

$$\text{Elasticity modulus: } E = 70{,}000\,\text{MPa},$$

$$\text{Poisson ratio: } \nu = 0.33, \quad \text{density: } \rho = 3.8E - 9t/\text{mm}^3.$$

In the structure design, both ends of the arc-shaped deformable shells are bonded with hinge to fabricate a driving component. The hinge connector in ABAQUS is utilized to simplify the physical hinge. The advantages of the simplification are as follows:

(1) Simulate the hinge characteristics (light quality and small volume) more accurately.

(2) Simulate the connection between hinge and laminates more easily.

In the simulation, the quality of the hinge is neglected, but superimposed in the supporting component correspondingly.

Tie constraints between each sleeve are utilized to ensure the avoidance of relative motion on the interface. Because each sleeve is closely connected to the other, rigid body displacement can be eliminated and interval can be greatly reduced if tie constraints are utilized in the whole process of modal analysis. The constraints of the supporting components and sleeves are also tie.

According to the description above, the three-longeron beam can be simplified as Fig. 2(a). The meshed beam is shown in Fig. 2(b).

The first six order vibration modes of the beam are shown in Fig. 3 where the longitudinal direction is established along z-axis.

The first- and second-order vibration modes are bending modes, the third mode is longitudinal mode with bulging, the fourth mode combines bulging and torsion modes, the fifth and sixth modes appear bending with bigger bending radius than that in first or second mode. The mode shapes of the three-longeron beam are similar to cantilever beam's, but there is a torsion deformation in the fourth mode. The main reason why torsion mode shape is significant is that the arc-shaped deformable shells contain degree of freedoms along x- and y-axes.

To study structure parameters that influence natural frequency of the beam, the modal analysis in several working conditions is utilized to make a comparison. The natural frequencies of the beam in different working conditions are shown in Table 4, and the working conditions are as follows:

Condition 1: The beam's simulation with original data;
Condition 2: Removing arc-shaped deformable shells;
Condition 3: The orientation angle of the composite layers is $30°/-30°$;
Condition 4: The orientation angle of the composite layers is $60°/-60°$;

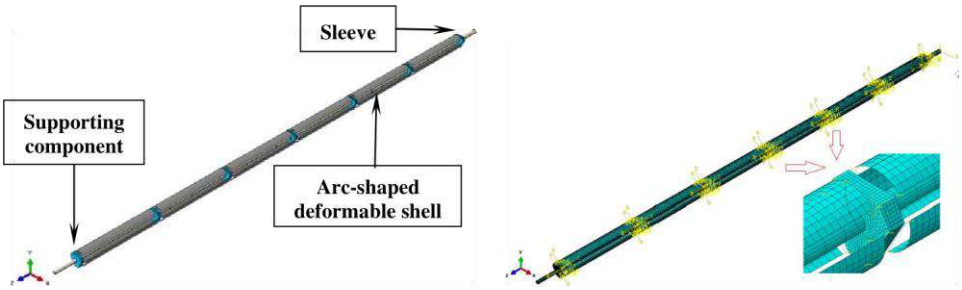

(a) (b)

Fig. 2. (a) The geometric model of three-longeron beam and (b) the mesh of three-longeron beam.

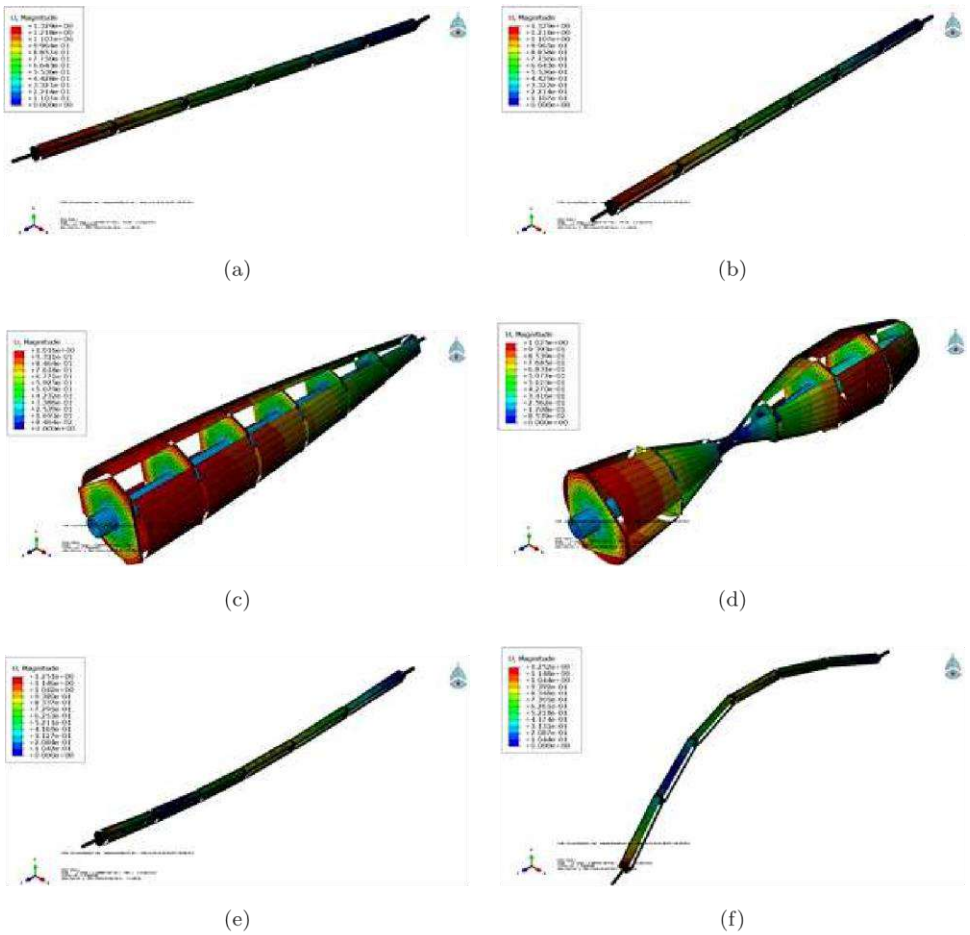

Fig. 3. The first six order vibration modes of the three-longeron beam. (a) The first-order vibration mode, (b) the second-order vibration mode, (c) the third-order vibration mode, (d) the fourth-order vibration mode, (e) the fifth-order vibration mode and (f) the sixth-order vibration mode.

Condition 5: The orientation angle of the composite layers is 90°/0°, meanwhile, the thickness of each layer is changed into 0.25 mm;
Condition 6: The orientation angle of the composite layers is 90°/0°, meanwhile, the thickness of each layer is changed into 0.75 mm.

From Table 4, the frequencies in working condition 2 and 5 increase obviously, on the contrary, the frequency in working condition 6 decreases significantly; meanwhile, the frequencies in working condition 3 and 4 are nearly the same with that in condition 1.

The conclusions can be obtained from Table 4. When the shells around the beam are removed, cross-sectional moment of inertia of the beam decreases, however, the

Table 4. The natural frequency of the three-longeron beam in different working conditions. Unit: Hz.

Working condition	First order	Second order	Third order	Fourth order	Fifth order	Sixth order
1	935.84	937.08	2279.2	6980	7882.1	7900.9
2	1468.2	1468.2	7861.6	7861.6	20,999	20,999
3	921.44	922.6	2282.3	6989.8	7655.3	7674.8
4	934.4	935.64	2219.8	6781	7859.9	7878.8
5	1366.9	1368.6	5090.8	14,283	14,324	15,363
6	715.27	716.21	1418.2	4459.8	4980.5	4991.1

first-order natural frequency increases to 1468.2 Hz, the increase in ratio reaches to 56% in working condition 2. The results in condition 3 and 4 indicate that changing orientation angle of the carbon fiber reinforced epoxy-based composite has little influence on natural frequency of the beam. The conditions 5 and 6 reveal that the natural frequency of the beam deceases with the increase of thickness of the layer, vice versa. The main reason may be attributed to the fact that the intermediate sleeves dominate the stiffness of the whole structure, the influence of the shells quality significantly decreases the natural frequency of the beam.

3. Modal Analysis of the Three-Longeron Truss

In order to increase the stiffness and stability of the three-longeron beam, the three-longeron truss is designed and analyzed. The truss built from three basic structural elements: intermediate shafts, which are made up of sleeves and parallel placed to the truss axis with their layout being triangle; arc-shaped deformable shells, which are connected to the intermediate shaft by supporting components; and battens, which are oriented transverse to the truss axis and connect the three intermediate shafts together.

The materials and dimensions of sleeves, arc-shaped deformable shells, and supporting components are the same as in Sec. 2. But the battens are acrylic plates with their sizes being 216 mm × 12 mm × 2 mm. The material parameters of acrylic plates are as follows:

$$\text{Elasticity modulus: } E = 2500\,\text{MPa},$$
$$\text{Poisson ratio: } \nu = 0.3, \quad \text{density: } \rho = 1.2E - 9t/\text{mm}^3.$$

The three-longeron truss can be simplified as Fig. 4(a). In ABAQUS, the battens can be simplified as shells, and the element type is S4R. The other components are established as in Sec. 2. The meshed truss is shown in Fig. 4(b). The first six order vibration modes of the truss are shown in Fig. 5.

The first- and second-order vibration modes are bending modes with small bending radius, the third mode is torsion mode, the fourth and fifth modes appear obvious bending mode; the sixth mode combines two torsion modes which are counter in the direction.

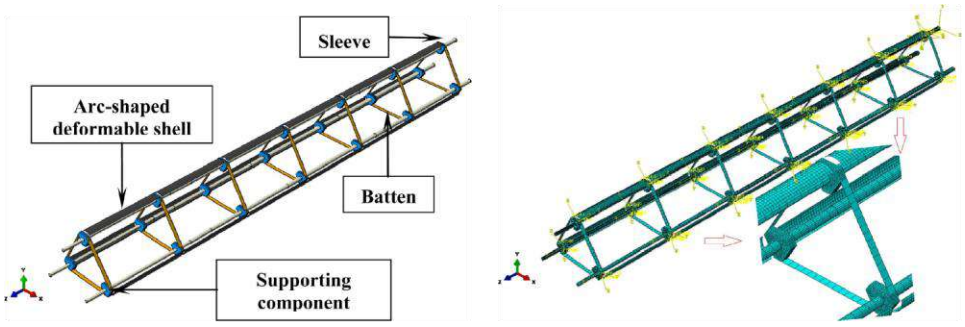

(a) (b)

Fig. 4. (a) The geometric model of three-longeron truss and (b) the mesh of three-longeron truss.

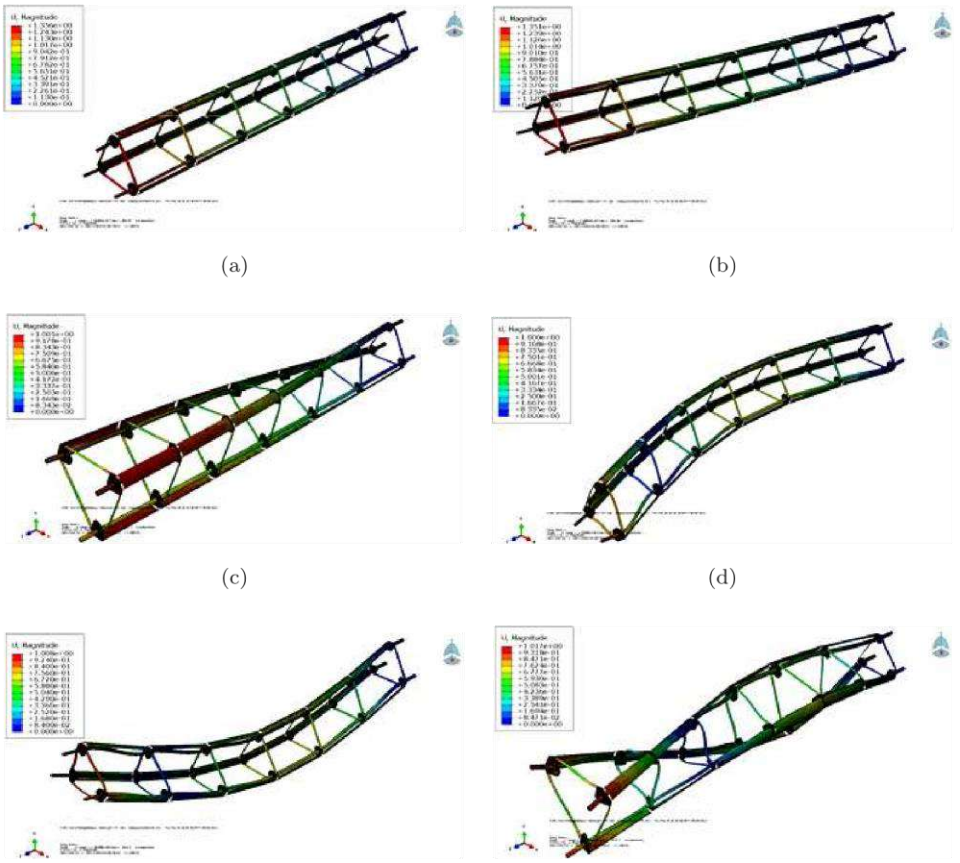

(a) (b)

(c) (d)

(e) (f)

Fig. 5. The first six order vibration modes of the three-longeron truss. (a) The first-order vibration mode, (b) the second-order vibration mode, (c) the third-order vibration mode, (d) the fourth-order vibration mode, (e) the fifth-order vibration mode and (f) the sixth-order vibration mode.

Table 5. The natural frequency of the three-longeron truss in different working conditions. Unit: Hz.

Working condition	First order	Second order	Third order	Fourth order	Fifth order	Sixth order
1	980.13	980.56	2155.30	5638.40	5644.70	6554.00
2	356.05	905.99	1032.20	1044.70	1435.00	1905.50
3	979.60	980.00	2092.80	5637.60	5643.90	6553.90
4	979.70	980.14	2161.50	5630.60	5636.90	6553.10
5	1319.00	1319.50	3094.50	6626.80	8537.80	8707.30
6	773.21	883.51	1446.70	3714.00	3717.60	4517.10
7	986.58	986.97	1848.00	4001.80	4934.90	5075.00
8	1334.70	1339.80	2056.90	5414.10	5421.20	6465.30

To study structure parameters that influence natural frequency of the truss, the modal analysis in several working conditions is utilized to make a comparison. The natural frequencies of the truss in different working conditions are shown in Table 5, and the working conditions are as follows:

Condition 1: The truss's simulation with original data;
Condition 2: Removing arc-shaped deformable shells around the sleeves;
Condition 3: The orientation angle of the composite layers is $30°/-30°$;
Condition 4: The orientation angle of the composite layers is $60°/-60°$;
Condition 5: The orientation angle of the composite layers is $90°/0°$, meanwhile, the thickness of each layer is changed into 0.25 mm;
Condition 6: The orientation angle of the composite layers is $90°/0°$, meanwhile, the thickness of each layer is changed into 0.75 mm;
Condition 7: The thickness of the acrylic plates is changed from 2 mm to 3 mm;
Condition 8: Substituting aluminum alloy plates for acrylic plates.

From Table 5, natural frequency of the truss in the working condition 2 decreases significantly, the frequency in working condition 6 decreases slightly; whereas, the frequencies in the 5 and 8 working conditions increase evidently; in conditions 3, 4 and 7, the frequencies remain almost the same with that in condition 1.

Comparing conditions 1 and 2, when the shells are removed, the first order of natural frequency decreases from 980.13 Hz to 356.05 Hz, and the decreased percentage is 64%. The first-order vibration mode shape in condition 2 is torsion, which is different from the bending mode in condition 1. The third mode in condition 2 is bending. The different mode shapes maybe caused by the absence of the shells, which will greatly increase the longitudinal stiffness of the truss. The conditions 3 and 4 indicate that the change of the orientation angle of the carbon fiber of composite has hardly effect on natural frequency. The conditions 5 and 6 illustrate that the effect of the thickness of layer has same tendency as that in Sec. 2. From conditions 3, 4, 5, and 6 in Secs. 2 and 3, we can drawn a conclusion that the quality of shell has bigger influence on the natural frequency than that of stiffness of shell, the increase of quality of shell reduce the natural frequency of structures. In addition,

conditions 7 and 8 reveal that the thickness change of the acrylic plate has little influence on natural frequency, but if the acrylic plate is replaced by aluminum alloy plate, the first-order frequency of the truss increases to 1334.7 Hz, and the increased percentage is 36%. Thereby, the increase in battens' stiffness can greatly increases the natural frequency.

4. Fabrication and Modal Test of the Three-Longeron Truss

Dimensions of the arc-shaped deformable shells are set as follows: length: 300 mm,

1640009-1

(a)

Fig. 8. Prototype of the three-longeron truss.

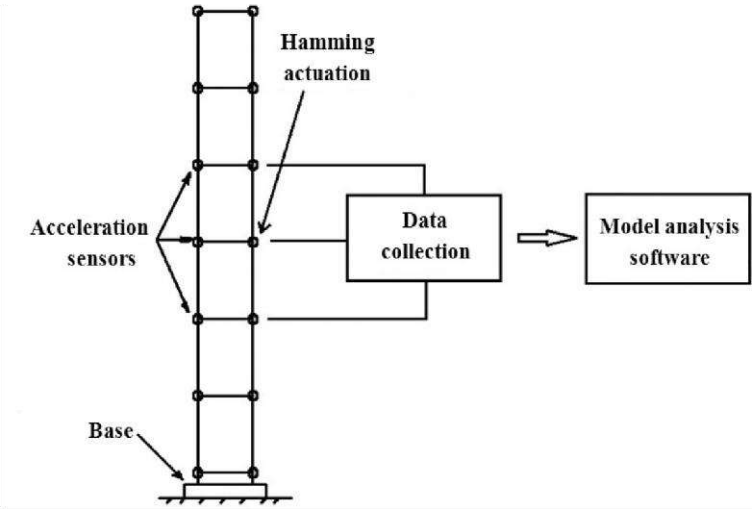

Fig. 9. Modal experiment system of the three-longeron truss.

It is inferred that the difference of the boundary conditions and contacts between the actual test and simulation results to the errors. In the simulation, the contacts of sleeves, as well as between supporting component and sleeve are all set to be tie contact. However, in the test the degree of adaptability of every contact is not that perfect. Because of the decrease of the constraints, the results of test are slightly smaller than simulation.

5. Conclusion

Feng, D. [2006] "Typical mast-liked deployment mechanism with truss structure," *Aerospace Shanghai* **1**, 009.

Fetchko, P., Sellers, J., Spanjer, G., Scherbarth, M., Winters, J., Barrett, R., Lake, M. and Keller, P. [2004] "Deployment optimization of a boom for FalconSAT-3 using elastic memory composite material," *18th Annual AIAA/USU Conference on Small Satellites*, Logan, Utah, USA, SSC04-VIII-4, pp. 1–10.

Gunes, I. S. and Jana, S. C. [2008] "Shape memory polymers and their nanocomposites, A review of science and technology of new multifunctional materials," *Journal of Nanoscience and Nanotechnology* **8**(4), 1616–1637.

Gunnar, T. [2002] "Deployable tensegrity structures for space applications," Stockholm, Royal Institute of Technology.

Hanayama, E., Kuroda, S., Takano, T., Kobayashi, H. and Kawaguchi, N. [2004] "Characteristics of the large deployable antenna on HALCA satellite in orbit," *IEEE Transacitons on Antenna and Propagation* **52**(7), 1777–1782.

Hu, J. L., Zhu, Y., Huang, H. H. and Lu, J. [2012] "Recent advances in shape memory polymers, structures, mechanism, functionality, modeling and applications," *Progress in Polymer Science* **37**(12), 1720–1763.

Im, E., Thomson, M., Fang, H. F., Pearson, J., Moore, J. and Lin, J. [2007] "Prospects of large deployable reflector antennas for a new generation of geostationary doppler weather radar satellites," *AIAA Space 2007 Conference and Exposition*, Long Beach, California, USA, AAIA 2007-9917, pp. 1–11.

Keller, P. N., Lake, M. S., Francis, W., Barrett, R., Wintergers, J., Harvey, J., Ruhl, E., Winter, J., . Scherbarth, M. R. and Murphey, T. W. [2004] "Development of a deployable boom for microsatellites using elastic memory composite material," *45thAIAA/ASME/ASCE/AHS/ASC Structures, Structural Dynamics and Materials Conference*, Palm Springs, California, USA, AAIA 2004-1603, pp. 1–9.

Kunzelman, J., Chung, T., Mather, P. T. and Weder, C. [2008] "Shape memory polymers with built-in threshold temperature sensors," *Journal of Material Chemistry* **18**(10), 1082–1086.

Leng, J. S., Lv, H. B., Liu, Y. J., Huang, W. M. and Du, S. Y. [2009] "Shape memory polymers — A class of novel smart materials," *MRS Bulletin* **34**(11), 848–855.

Leng, J. S., Lan, X., Liu, Y. J. and Du, S. Y. [2011] "Shape memory polymers and their composites, stimulus methods and applications," *Progress in Materials Science* **56**(7), 1077–1135.

Li, F. F., Liu, L. W., Lan, X., Zhou, X. J., Bian, W. F., Liu, Y. J. and Leng, J. S. [2016] "Preliminary design and analysis of a cubic deployable support structure based on shape memory polymer composite," *International Journal of Smart and Nano Materials* **7**(2), 106–118.

Lillie, C. [2005] "Large deployable telescopes for future space observatories," *Optics & Photonics 2005. International Society for Optics and Photonics*, San Diego, California, USA, 58990D, pp. 1–12.

Liu, Y. J., Du, H. Y., Liu, L. W. and Leng, J. S. [2014] "Shape memory polymers and their composites in aerospace applications, a review," *Smart Materials and Structures* **23**(2), 023001.

Luo, Y. and Duan, B. Y. [2005] "The study on structure of space deployed antenna," *Electro-Mechanical Engineering* **21**(5), 1–5.

Lv, H. B., Yu, K., Sun, S. H., Liu, Y. J. and Leng, J. S. [2010] "Mechanical and shape memory behavior of shape memory polymer composites with hybrid fillers," *Polymer International* **59**(6), 766–771.

Mather, P. T., Luo, X. F. and Rousseau, I. A. [2009] "Shape memory polymer research," *Annual Review of Materials Research* **39**, 445–471.

Meng, Q. B. and Hu, J. L. [2009] "A review of shape memory polymer composites and blends," *Composites Part A-Applied Science and Manufacturing* **40**(11), 1661–1672.

Mori, O., Sawada, H., Hanaoka, F., Kawaguchi, J., Shirasawa, Y., Sugita, M., Miyazaki, Y., Sakamoto, H. and Funase, R. [2009] "Development of deployment system for small size solar sail mission," *Transactions of the Japan Society for Aeronautical and Space Sciences, Space Technology Japan* **7**(ists26), Pd_87–Pd_94.

Oegerle, W., Purves, L., Budinoff, J., Moe, R., Carnahan, T., Evans, D. and Kim, C. [2006] "Concept for a large scalable space telescope: In-space assembly," *SPIE Astronomical Telescopes+ Instrumentation*, International Society for Optics and Photonics, Orlando, Florida, USA, 62652C, pp. 1–12.

Ohki, T., Ni, Q. Q., Ohsako, N. and Iwamoto, M. [2004] "Mechanical and shape memory behavior of composites with shape memory polymer," *Composites Part A-Applied Science and Manufacturing* **35**(9), 1065–1073.

Pollard, E. L., Murphey, T. W. and Sanford, G. E. [2007] "Experimental and numerical analysis of a DECSMAR structure's deployment and deployed performance," Air Force Research Laboratory, Space Vehicles Directorate.

Ratna, D. and Karger-Kocsis, J. [2008] "Recent advances in shape memory polymers and composites: A review," *Journal of Material Science* **43**(1), 254–269.

Richard, C. G. [1995] "Potential future applications for the tracking and data relay satellite II [TDRS II] system," *Acta Astronautica* **35**(8), 537–545.

Takano, T., Miura, K., Natori, M., Hanayama, E., Inoue, T., Noguchi, T., Miyahara, N. and Nakaguro, H. [2004] "Deployable antenna with 10-m maximum diameter for space use," *IEEE Transacitons on Antenna and Propagation* **52**(1), 2–11.

Tsuda, Y., Mori, O., Funase, R., Sawada, H., Yamamoto, T., Saiki, T., Endo, T., Yonekura, K., Hoshino, H. and Kawaguchi, J. [2013] "Achievement of IKAROS — Japanese deep space solar sail demonstration mission," *Acta Astronautica* **82**(2), 183–188.

Wei, Z. G., Sandstrom, R. and Miyazaki, S. [1998] "Shape memory materials and hybrid composites for smart systems-Part II shape memory hybrid composites," *Journal of Materials Science* **33**(15), 3763–3783.

Wie, B., Furumoto, N., Banerjee, A. and Barba, P. [1986] "Modeling and simulation of spacecraft solar array deployment," *Journal of Guidance, Control, and Dynamics* **9**(5), 593–598.

Xie, T. [2010] "Tunable polymer multi-shape memory effect," *Nature* **464**(7286), 267–270.

Zhang, R. R., Guo, X. G., Liu, Y. J. and Leng, J. S. [2014] "Theoretical analysis and experiments of a space deployable truss structure," *Composite Structures* **112**, 226–230.

Zhou, B. and Liu, Y. J. [2009] "A glass transition model for shape memory polymer and its composite," *International Journal of Modern Physics B* **23**(6–7), 1248–1253.